Structure determination of hydrogen-terminated 4*H*-SiC(0001) by LEED

Hiroshi Ando,[1,*] Anton Visikovskiy,[1] Takeshi Nakagawa,[2] Seigi Mizuno,[2] and Satoru Tanaka[1]
[1]*Department of Applied Quantum Physics and Nuclear Engineering, Kyushu University, Fukuoka 819-0395, Japan*
[2]*Department of Molecular and Material Sciences, Kyushu University, Kasuga, Fukuoka 816-8580, Japan*

(Received 24 February 2019; published 28 June 2019)

SiC(0001)-(1 × 1)-H consisting of monohydride is a preferred starting surface structure for synthesis of the two-dimensional materials on SiC(0001). Here we report preparation of the SiC(0001)-(1 × 1)-H by atomic hydrogen exposure and structure determination of the SiC(0001)-(1 × 1)-H by a quantitative LEED analysis. Our data show that the SiC(0001)-(1 × 1)-H is indeed a bulk terminated unreconstructed SiC(0001) surface. The sample morphology was also investigated using AFM. The dominance of one of two possible inequivalent surface terminations of 4*H* polytype of SiC crystal was confirmed.

DOI: 10.1103/PhysRevB.99.235434

I. INTRODUCTION

Silicon carbide (SiC) is a wide-gap semiconductor and a promising material for high-power and high-frequency devices. Recently, it is also considered as a very convenient substrate for new two-dimensional (2D) materials (examples are graphene [1], Sn triangular lattice atomic layer (TLAL) [2,3], bismuthene [4], and others). This is due to the high temperature stability allowing high temperature growth without significant degradation of the surface, convenient unit cell size [noticeably smaller than conventional Si(111) surface, and a lot of 2D materials exhibit hexagonal cell of ∼3 Å], and a wide band gap which is important both for device application and for research purpose, as it allows one to clearly observe low-energy band structure of 2D overlayer by experimental methods.

Hydrogen surface termination is very important for the above mentioned applications. Hydrogen saturating surface dangling bonds passivate the surface making it nonreactive, stable even for air exposure, and remove electronic surface states in the band gap. For the sake of 2D material synthesis it is important that hydrogen keep the surface stoichiometric (relevant in the case of SiC, where most surface reconstructions are either Si or C rich, which may result in defect incorporation into 2D overlayer lattice and/or parasitic doping), reduces the diffusion barriers, and, also, could be removed at relatively low temperatures (by annealing at temperatures lower than those for Si adatoms desorption, or even at room temperature using light [5–7]). Thus the use of hydrogenated SiC(0001) as a starting surface is much more desirable than the typical SiC(0001)-$(\sqrt{3}\times\sqrt{3})R30^{\circ}$-Si consisting of Si adatoms in T_4 sites (further $\sqrt{3}$-Si) [8,9]. The latter is a clean and extremely stable reconstruction appearing after ultrahigh vacuum (UHV) cleaning and treatment of SiC(0001) surface which, until now, has often served as a starting point for overlayer growth. There have been reported cases, however, when $\sqrt{3}$-Si prevented the growth of 2D materials. For example, Sn TLAL structure, showing unique electronic properties, could not be grown from $\sqrt{3}$-Si surface despite the fact that DFT calculations predicted its stability on bare SiC(0001) [2,3,10]. So, to date, it could only be generated by Sn intercalation into graphene/SiC(0001) interface, which is free of Si adatoms. The same could be said about recently synthesized bismuthene, which was grown from hydrogenated SiC(0001), but not from $\sqrt{3}$-Si [4]. Surprisingly, the number of studies on SiC(0001) hydrogenation is relatively few.

Despite the many similarities in properties of the final hydrogenated surface, SiC{0001} surfaces cannot be easily hydrogenated by wet chemical processing the same as well studied Si(111). Methods to produce hydrogen-terminated SiC(0001) can be roughly classified into two approaches. One is annealing SiC(0001) at high temperatures (>1000 °C) in ultrapure H_2 gas at atmospheric pressure [5–7,11–15] (CVD method). This method requirement of ultrapure (⩾8.0 purity) hydrogen makes it quite expensive, and the need to transfer the sample from CVD chamber into vacuum for further processing and analysis may introduce some contaminations. So, this method is more suited for industrial application and device fabrication processes. The comprehensive review on the properties of the resultant surface was written by Seyller [5]. Another approach utilizes the surface exposure to atomic hydrogen or hydrogen plasma in a UHV chamber [16–21] (UHV method). This could be advantageous for laboratory use to study surface phenomena *in situ* keeping the surface free of contaminations, because this method is cheap and simple, and does not require *ex situ* transfer. In either method, a (1 × 1) phase of hydrogen-terminated SiC(0001) was observed, and was primarily studied by spectroscopy [Fourier transform infrared (FTIR) spectroscopy [11–13], x-ray photoelectron spectroscopy (XPS) [14], angle-resolved photoemission spectroscopy (ARPES) [6,7,15], and high-resolution electron energy-loss spectroscopy (HREELS) [17,20], and others] or low-energy electron diffraction (LEED) from the symmetry point of view.

Here we would like to point out that processes occurring during hydrogenation, the resultant hydrogenated surface structure, and its morphology may significantly differ for

*h.ando@kyudai.jp

the two methods described above. In the CVD method high temperature enhances surface mobility and overall atoms dynamics, and atmospheric gas pressure suppresses desorption. In the UHV method, quite oppositely, lower temperatures, vacuum conditions, and highly reactive atomic hydrogen result in enhanced surface reaction and lower atoms mobility, which may lead to formation of more complicated hydrogen containing reconstructions still exhibiting (1×1) periodicity. There are reports of incompletely hydrogenated surfaces, surfaces containing -OH terminations, and even surfaces with on-top -SiH_3 terminations all exhibiting (1×1) diffraction patterns [18,20]. While most of the previous studies were done on hydrogenation by the CVD method, and it can be relatively safely assumed that this method works well to produce true SiC(0001)-(1×1)-H [further (1×1)-H] termination, one cannot say so about the UHV method. So, the structure determination by means of a highly sensitive technique, such as structural LEED analysis, is highly important, but has not been reported on the (1×1)-H (even grown by the CVD method) to our knowledge. Another important point is that the majority of previous studies have been done on 6*H*-SiC(0001), and not much information especially on step morphology and surface stacking order is known about 4*H* polytype. Our study is aiming at addressing all these issues.

In this study, we present the structural determination of the (1×1) phase of the hydrogen-terminated SiC(0001) by quantitative LEED analysis. Our data show that the (1×1)-H consists of a bulk-truncated unreconstructed SiC(0001) surface (with monohydride). Moreover, by LEED and atomic force microscopy (AFM), we confirmed the dominance of one of two possible inequivalent surface terminations of 4*H* polytype of SiC crystal for our (1×1)-H samples prepared by the UHV method. In 2D materials, electronic structures depend on surface structure of the materials directly, so previous spectroscopic study and our present structural study are complementary.

II. EXPERIMENT

An on-axis commercially available 4*H*-SiC(0001) substrate was treated by H_2 gas at 1360 °C for 15 min in atmospheric pressure (H_2 etching) in a cold-wall reactor of a quartz furnace. This process enables one to remove scratches and contaminations from the sample surface. The sample was then transferred into a UHV chamber (base pressure $<1 \times 10^{-8}$ Pa) and degassed by direct current heating at 600 °C for at least 12 h. The temperature of the sample was measured using an infrared pyrometer with an emissivity setting of 0.56.

After degassing the surface showed faint $(\sqrt{3} \times \sqrt{3})R30^\circ$ structure [shown in Fig. S1 [22]], which indicates incomplete formation of well-known silicate adlayers [23,24]. The silicate adlayers were then annealed at 1050 °C for 5–10 min, resulting in formation of $\sqrt{3}$-Si. The transition to $\sqrt{3}$-Si could be confirmed by means of sharpness of reflection high-energy electron diffraction (RHEED) streaks and change in LEED $I(E)$ profiles. Also, we could confirm the formation of the $\sqrt{3}$-Si by structural LEED $I(E)$ analysis (not shown here).

After the $\sqrt{3}$-Si formation, the sample was cooled down to 400−500 °C and exposed to atomic hydrogen for 15 min. This results in changing the LEED pattern to sharp (1×1). We confirmed that the clear (1×1) pattern appears also after atomic hydrogen exposure of the sample cooled down to room temperature (RT). However, in RT experiments, as reported previously, a significant amount of di- and trihydride species may appear on the surface [18]. On the other hand, in experiments with atomic deuterium exposure at 430 °C, monodeuteride prevail [20]. So, we preferred to use elevated temperatures in our experiments. Note, however, that the temperatures are still significantly lower than those used in the CVD hydrogenation method. Atomic hydrogen was produced by cracking H_2 molecules by a hot tungsten filament in the UHV chamber. The temperature of the tungsten filament was presumed to be approximately 1600 °C and the distance from the sample surface was ∼5 cm. The resultant surface was studied by LEED while being cooled to liquid nitrogen temperature and by AFM *ex situ*.

The LEED patterns at the incident electron energies in the range of 50–500 eV (1 eV step) were recorded using a digital charge-coupled device (CCD) camera with a homemade computer controlled data acquisition system.

The intensity of symmetry equivalent spots has been averaged to negate measurement and alignment errors. The total energy range of inequivalent $I(E)$ curves, $\Delta E = 2016$ eV. A Barbieri–Van Hove symmetrized automated tensor LEED (SATLEED) package was used to determine the atomic positions [25]. The initial optimal atomic positions for each model were provided by density functional theory (DFT) calculation using Vienna *ab initio* simulation package (VASP) [26].

For tensor LEED analysis the electron scattering was represented using seven electron wave phase shifts. The damping of incident elastic electron flux was represented by the imaginary part of the inner potential, $V_{0i} = -5.0$ eV, with Pendry's reliability factor (R_P) used to judge the fitting quality and direct the automated search algorithm [25,27]. The best agreement between experimental and calculated $I(E)$ curves was determined by minimizing R_P, with errors in the structural parameters estimated from the variance of R_P, $\Delta R_P = R_{P,\min} \sqrt{8|V_{0i}|/\Delta E}$ [27].

To investigate desorption of hydrogen from the hydrogen-terminated sample and the resultant change of the surface structure, RHEED patterns were collected using a similar automated system while raising the temperature of the sample intermittently (a heating rate of 20 °C/5 min). The RHEED patterns were captured from $[1\bar{1}00]$ direction. The desorption experiment has been carried in a separate RHEED chamber after *in situ* sample preparation. For comparison, a hydroxyl-terminated sample [further (1×1)-OH] treated by wet-chemical etching using 46% hydrofluoric acid (HF) [28] was also investigated.

III. RESULTS AND DISCUSSION

In Fig. 1, AFM topography images of SiC surface after (a) H_2 etching and (b) after exposure to atomic hydrogen are shown. Red and blue lines indicate cross-sectional height profiles across and parallel to the steps of SiC, respectively. Insets show magnified images of surface terrace(s). After H_2 etching a typical step-terrace feature is observed. As seen in the height profile *a1*, step height is 0.5 nm, equivalent to

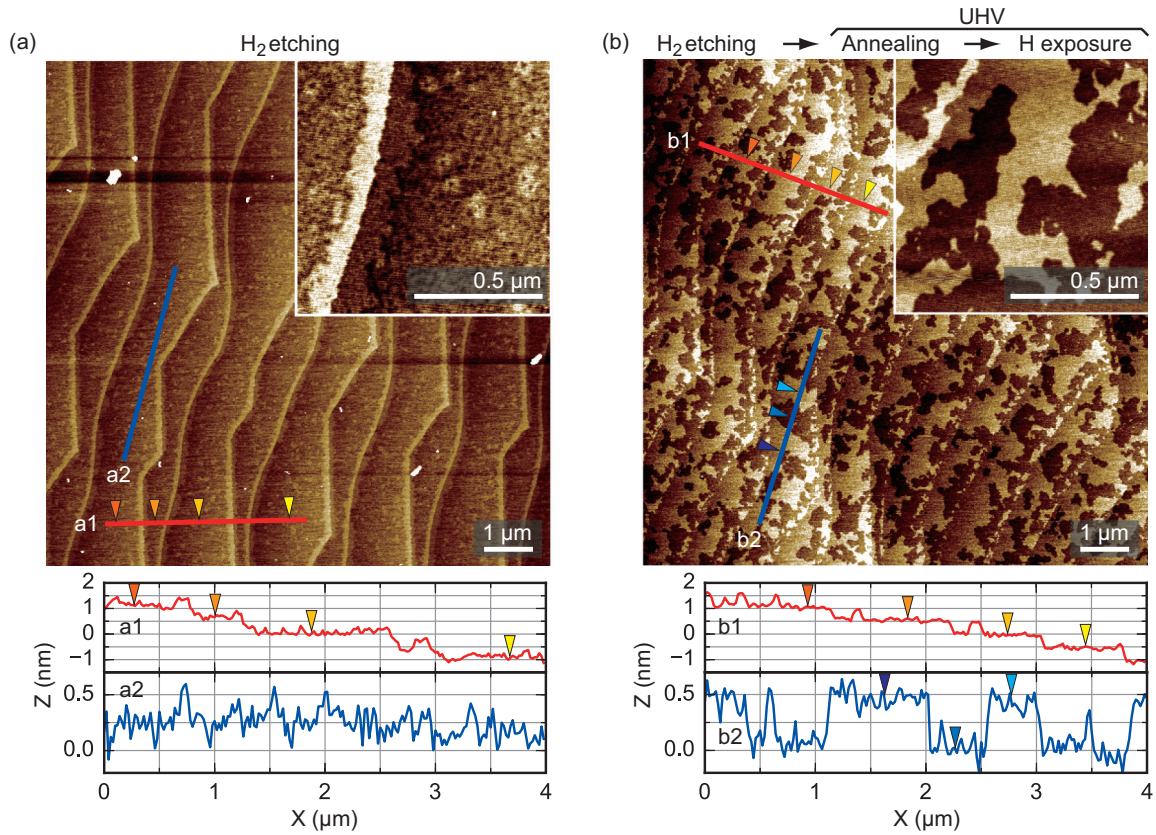

FIG. 1. AFM topography images of SiC surfaces after (a) H_2 etching and (b) annealing and atomic hydrogen exposure in UHV. Red (blue) lines are line profiles across (parallel to) the step of SiC. (a) After H_2 etching, steps with a height of two SiC bilayer appear. The surface is covered with silicate. (b) After annealing and atomic hydrogen exposure in UHV, silicate was removed.

half-unit cell length of c axis of 4H-SiC. The mechanism of the step bunching formation and zigzag shape of the steps was discussed in [29–32]. The terrace area shows some roughness, probably due to the formation of silicate adlayers. The stripelike features at the terrace edges, 0.5 nm in height, may also originate from oxides, but are not yet identified. After the surface annealing and exposure to atomic hydrogen, the appearance changes to a "moth-eaten" like surface, as shown in Fig. 1(b). This could be caused by local etching by atomic hydrogen initiating from defects on terraces (see discussion in Supplemental Material [22]). The typical height of the pits remaining after hydrogen exposure is 0.5 nm [see the cross-sectional profile *b2* in Fig. 1(b)], again half-unit cell height. The terrace appears much smoother compared to the oxidized surface.

In 4H polytype of SiC there are four possible surface terminations: S1 ($BCBA\ldots$), S2 ($ABCB\ldots$), S1* ($BABC\ldots$), and S2* ($CBAB\ldots$) [33] (and see Fig. 5 also). S1 and S1* are equivalent to each other with symmetry inversion and occur in half-unit cell steps in 4H-SiC; the same is true for S2 and S2*. S1/S1* and S2/S2* are principally different in terms of the stacking fault depth and thus have different surface energy (unreconstructed S2 termination being 15 meV/cell more stable than S1 according to DFT results [22]). Areal occupation of domains with inequivalent surface terminations depends on the preparation method and surface reconstruction [8,33].

Since the AFM image shows only half-unit cell steps, there should be one dominant inequivalent termination, whether its S1/S1* or S2/S2*. According to AFM the areal occupation of direct and inverted (starred) domain is approximately 50%/50%. This stacking configuration influences LEED $I(E)$ curves since the diffraction is affected by the subsurface stacking order and should be taken into account for structure determination when the R_P is calculated, as will be discussed later.

Figures 2 and S1 [22] show LEED patterns of the $\sqrt{3}$-Si SiC(0001) surface (a) before and (b) after atomic hydrogen exposure. $\sqrt{3}$ spots disappeared and sharp (1 × 1) spots without significant background were recognized. The LEED pattern has sixfold symmetry [22], which is in agreement with AFM observations of approximately equal areal occupation of domains with symmetry inversion.

The possible atomic models to explain this (1 × 1) surface are shown in Fig. 3. Figures 3(a)–3(c) indicate the (1 × 1)-H model, the (1 × 1)-OH model, and a (1 × 1)-SiH model, respectively. The (1 × 1)-OH model is known as a hydroxyl-terminated (1 × 1) surface appearing after HF treatment of the SiC(0001) [28,33–38]. The (1 × 1)-SiH model is justified by the presence of excess Si atoms on the surface and also serves a purpose as a gauge to check validity of R_P. In the (1 × 1)-SiH model, Si atoms are put on T_1 sites of the SiC(0001) surface. It has to be noted that existence of T_1 Si atoms in the form of Si-H_3 radicals on hydrogenated

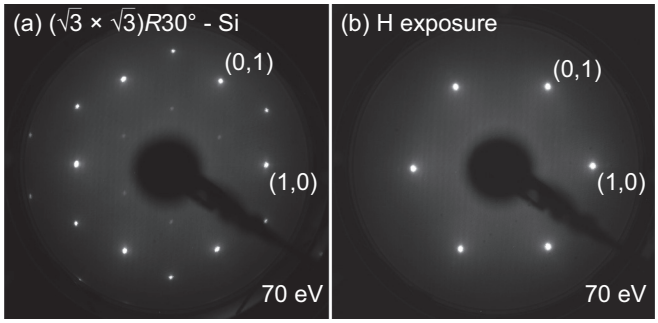

FIG. 2. LEED patterns of (a) before and (b) after atomic hydrogen exposure of $\sqrt{3}$-Si.

SiC(0001) has been also proposed previousely [18]. As LEED is not sufficiently sensitive to H atoms positions owing to a small electron scattering cross section of hydrogen atoms, we can also check the existence of Si-H_3 radicals indirectly by (1 × 1)-SiH model.

Because hydrogen atoms are difficult to detect by electron diffraction, calculated $I(E)$ curves of a bulk terminated unreconstructed SiC(0001) surface without H termination led to almost the same R_P as the (1 × 1)-H. Therefore, hydrogen atom position was not optimized by LEED analysis and H atoms were fixed at a height determined by DFT calculation.

The experimental LEED $I(E)$ curves of diffraction spots are shown by black lines in Fig. 4. Symmetrically equivalent spots have been averaged, also, as the diffraction pattern showed sixfold rotational symmetry; spots related by 180° rotation have also been averaged. Using the models above, the structural parameters have been optimized in order to obtain the best fit of theoretical $I(E)$ curves to experimental ones. As a result, the (1 × 1)-H model gives a smallest R_P (= 0.13) and best $I(E)$ fitting as indicated by orange lines in Fig. 4, whereas the R_P of the other models are larger than

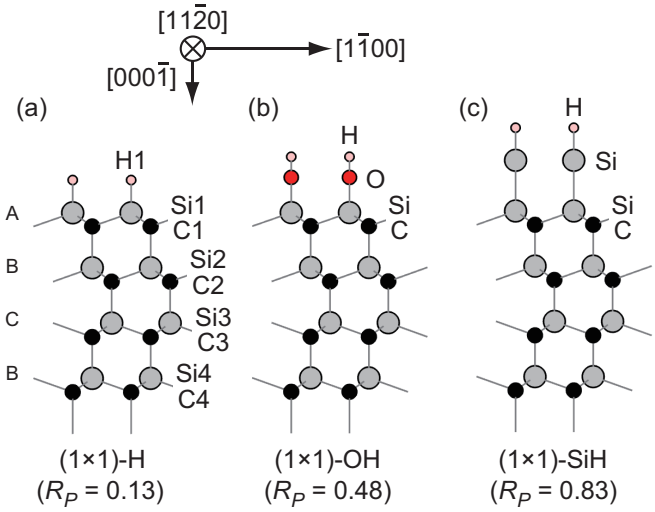

FIG. 3. Side views of examined structure models. (a) (1 × 1)-H, (b) (1 × 1)-OH, and (c) Si atoms are put on T_1 sites of the SiC(0001). The models were assumed as S2 type stacking. The calculated $I(E)$ curves of the (1 × 1)-H model is in good agreement with experimental $I(E)$ curves with small R_P.

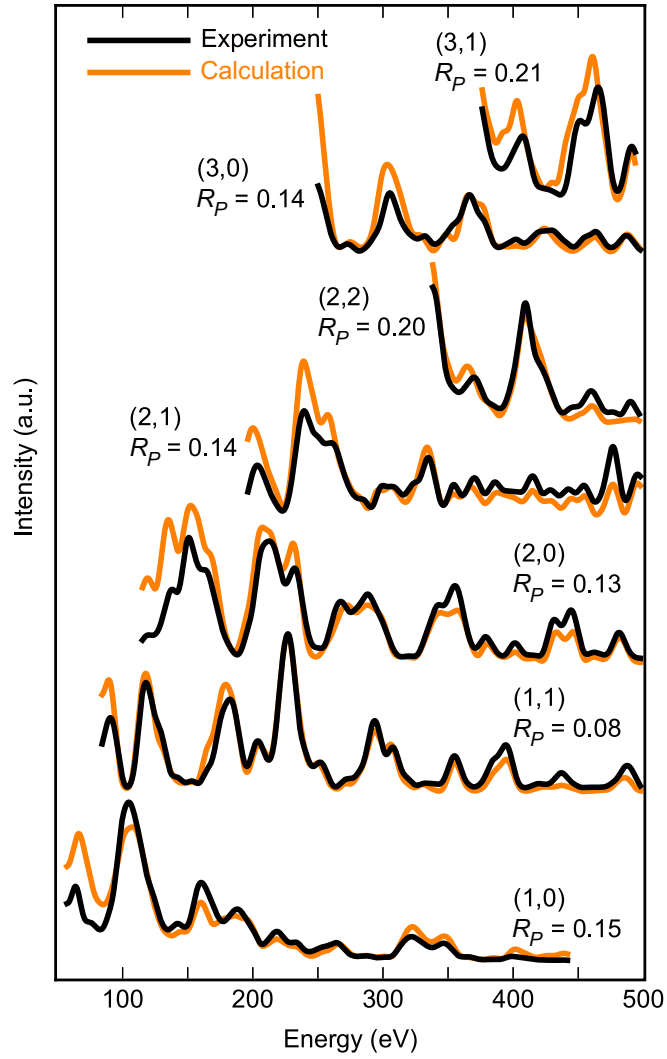

FIG. 4. Experimental (black lines) and best-fit calculated (orange lines) $I(E)$ curves for the (1 × 1)-H. Total R_P is 0.13.

0.40. Atomic coordinates of the best-fit (1 × 1)-H model are shown in Table I. The minimum R_P (= 0.13) is obtained assuming S2 surface termination and averaging $I(E)$ intensity of symmetrically equivalent spots assuming 50%/50% S2 and S2* domains ratio. The possibility of S1/S1* terminations has been ruled out because of large R_P (= 0.53) (Fig. 5).

From the above results, it is confirmed that the surface structure prepared by the UHV method is indeed a bulk terminated unreconstructed SiC(0001) surface terminated with hydrogen atoms. On the other hand, the R_P value of (1 × 1)-SiH model is significantly higher. So, the LEED analysis is quite sensitive to the existence of T_1 Si adatoms. This fact rules out the possibility of a significant amount of random di- and trihydride species on a hydrogenated surface, as otherwise we would not be able to obtain sufficiently low R_P.

The S1 and S2 domain concentration was also investigated by LEED analysis. The calculated $I(E)$ spectra of a mixed surface composed of two domains was defined as

$$I_{\mathrm{mix}}(E) = (1-\alpha)I_{S1}(E) + \alpha I_{S2}(E), \quad (1)$$

TABLE I. Atomic coordinates of the best-fit (1 × 1)-H model. The corresponding labels of atoms are shown in Fig. 3(a). Single asterisks (*) indicate the symmetrically fixed positions. Double asterisk (**) indicates that the position of hydrogen atom is fixed with the value calculated by DFT calculation. Lattice constant of SiC, $a_{SiC} = 3.081_{\pm 0.016}$.

Labels	$[000\bar{1}]$ (Å)	Δz (Å)	$[1\bar{1}00]$ (Å)	$[11\bar{2}0]$ (Å)	T_{Debye} (K)
H1	0**		0*	0*	220
Si1	$1.50_{\pm 0.01}$	1.50	0*	0*	310
C1	$2.11_{\pm 0.04}$	0.61	$\frac{1}{2\sqrt{3}}a_{SiC}$*	$\frac{1}{2}a_{SiC}$*	520
Si2	$4.01_{\pm 0.02}$	1.90	$\frac{1}{2\sqrt{3}}a_{SiC}$*	$\frac{1}{2}a_{SiC}$*	380
C2	$4.62_{\pm 0.04}$	0.61	$\frac{1}{\sqrt{3}}a_{SiC}$*	0*	570
Si3	$6.51_{\pm 0.03}$	1.89	$\frac{1}{\sqrt{3}}a_{SiC}$*	0*	670
C3	$7.13_{\pm 0.06}$	0.62	$\frac{1}{2\sqrt{3}}a_{SiC}$*	$\frac{1}{2}a_{SiC}$*	720
Si4	$9.04_{\pm 0.02}$	1.91	$\frac{1}{2\sqrt{3}}a_{SiC}$*	$\frac{1}{2}a_{SiC}$*	670
C4	$9.67_{\pm 0.06}$	0.63	0*	0*	720

where $I_{S1}(E)$, $I_{S2}(E)$, and α are calculated $I(E)$ spectra of S1, S2, and the ratio of S2 domain, respectively. The simple intensity superposition formula is justified as the domains observed by AFM have size significantly larger than typical LEED coherence length (10–50 nm). In Fig. 5, R_P is plotted against the domain concentration of S2 based on Eq. (1). When $\alpha = 91\%$, R_P takes the minimum value. Therefore, S2 domain prevalence was confirmed.

Figures 6(a) and 6(b) show RHEED patterns of (1 × 1)-H sample during postannealing at 450 °C and 650 °C, respectively. In Fig. 6(b) third order reflexes appear indicating desorption of H atoms and restoration of $\sqrt{3}$-Si phase. Figure 6(c) shows data series of the RHEED spots intensities vs annealing temperature. When the sample temperature is over 600 °C, the intensities of 1/3 spots start to increase rapidly, indicating

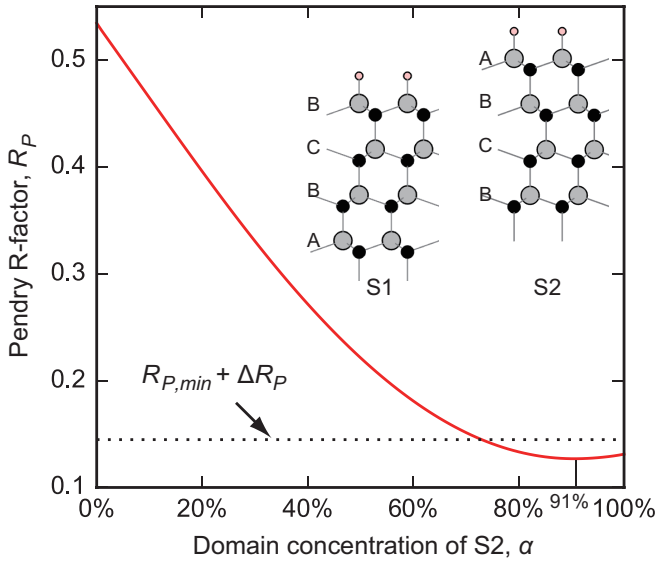

FIG. 5. R_P plotted against domain concentration of S2. When domain concentration of S2, $\alpha = 91\%$, R_P takes the minimum value.

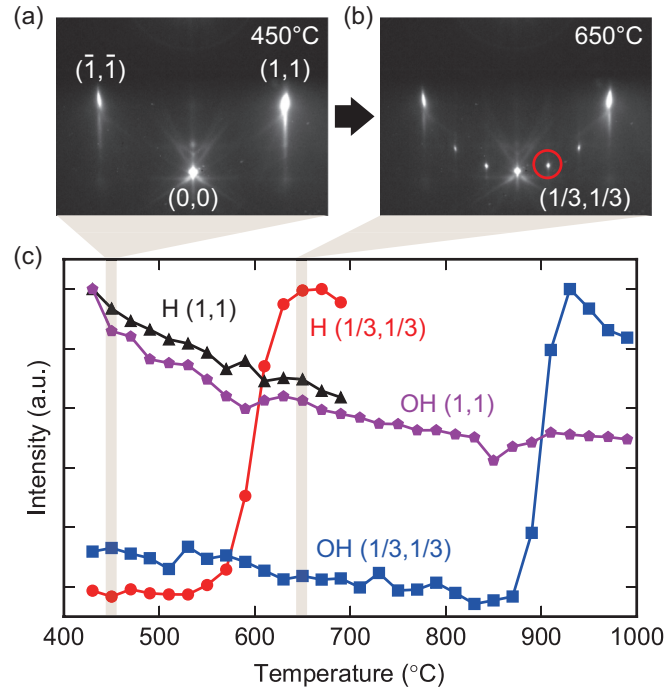

FIG. 6. Changes in RHEED patterns by annealing. RHEED patterns when the (1 × 1)-H sample was annealed at (a) 450 °C and (b) 650 °C. (c) RHEED intensity changes. Pattern of the (1 × 1)-H changes at around 600 °C to $(\sqrt{3} \times \sqrt{3})R30°$. On the other hand, the (1 × 1)-OH changes at around 900 °C.

massive H desorption. On the other hand, the (1 × 1)-OH reconstruction of the HF treated test sample changes to $\sqrt{3}$-Si at around 900 °C due to much stronger Si-O bonding. These desorption temperatures are in good agreement with the values reported in [5,14,35,36] that were investigated by LEED and FTIR. The desorption temperature of the (1 × 1)-H was also investigated in detail using temperature programed desorption (TPD) in [19,21]. This agreement provides more evidence that our method produces a true (1 × 1)-H surface.

IV. CONCLUSION

In this paper, we discussed the structural aspect of the SiC(0001)-(1 × 1)-H surface reconstruction by quantitative LEED analysis and AFM. The $\sqrt{3}$-Si structure was changed to the (1 × 1)-H by atomic hydrogen exposure of a sample held at 400–500 °C. Since the LEED $I(E)$ curve fitting resulted in sufficiently low R_P, it was confirmed that our (1 × 1)-H sample is indeed represented by bulk truncated unreconstructed SiC(0001) surface terminated with on-top hydrogen atoms. Our analysis rules out the existence of a noticeable amount of -OH and -SiH_x radicals on the surface, which confirms that this preparation method results in a high-quality hydrogenated surface suitable for easy growth of 2D materials by means of molecular beam epitaxy. Additionally, AFM topography measurements have shown that SiC surface is etched by atomic hydrogen exposure with pits depth of half unit cell of 4*H*-SiC. Therefore, one of two possible inequivalent surface terminations (hexagonal or cubic) of 4*H* polytype of SiC crystal, namely S2 (cubic), dominate on our sample.

[1] C. Berger, Z. Song, X. Li, X. Wu, N. Brown, C. Naud, D. Mayou, T. Li, J. Hass, A. N. Marchenkov, E. H. Conrad, P. N. First, and W. A. de Heer, Science **312**, 1191 (2006).

[2] S. Hayashi, A. Visikovskiy, T. Kajiwara, T. Iimori, T. Shirasawa, K. Nakastuji, T. Miyamachi, S. Nakashima, K. Yaji, K. Mase, F. Komori, and S. Tanaka, Appl. Phys. Express **11**, 015202 (2018).

[3] A. Visikovskiy, S. Hayashi, T. Kajiwara, F. Komori, K. Yaji, and S. Tanaka, arXiv:1809.00829.

[4] F. Reis, G. Li, L. Dudy, M. Bauernfeind, S. Glass, W. Hanke, R. Thomale, J. Schäfer, and R. Claessen, Science **357**, 287 (2017).

[5] T. Seyller, J. Phys.: Condens. Matter **16**, S1755 (2004).

[6] K. V. Emtsev, T. Seyller, L. Ley, L. Broekman, A. Tadich, J. D. Riley, R. G. C. Leckey, and M. Preuss, Phys. Rev. B **73**, 075412 (2006).

[7] K. V. Emtsev, T. Seyller, L. Ley, A. Tadich, L. Broekman, J. D. Riley, R. C. G. Leckey, and M. Preuss, Surf. Sci. **600**, 3845 (2006).

[8] U. Starke, J. Schardt, J. Bernhardt, M. Franke, and K. Heinz, Phys. Rev. Lett. **82**, 2107 (1999).

[9] A. Coati, M. Sauvage-Simkin, Y. Garreau, R. Pinchaux, T. Argunova, and K. Aïd, Phys. Rev. B **59**, 12224 (1999).

[10] K. Yaji, A. Visikovskiy, T. Iimori, K. Kuroda, S. Hayashi, T. Kajiwara, S. Tanaka, F. Komori, and S. Shin, Phys. Rev. Lett. **122**, 126403 (2019).

[11] H. Tsuchida, I. Kamata, and K. Izumi, Jpn. J. Appl. Phys. **36**, L699 (1997).

[12] H. Tsuchida, I. Kamata, and K. Izumi, Appl. Phys. Lett. **70**, 3072 (1997).

[13] H. Tsuchida, I. Kamata, and K. Izumi, J. Appl. Phys. **85**, 3569 (1999).

[14] N. Sieber, T. Seyller, L. Ley, D. James, J. D. Riley, R. C. G. Leckey, and M. Polcik, Phys. Rev. B **67**, 205304 (2003).

[15] S. Glass, F. Reis, M. Bauernfeind, J. Aulbach, M. R. Scholz, F. Adler, L. Dudy, G. Li, R. Claessen, and J. Schäfer, J. Phys. Chem. C **120**, 10361 (2016).

[16] V. van Eisbergen, O. Janzen, and W. Mönch, Mater. Sci. Eng. B **46**, 366 (1997).

[17] C. R. Stoldt, C. Carraro, and R. Maboudian, Surf. Sci. **466**, 66 (2000).

[18] T. Fujino, T. Fuse, J. T. Ryu, K. Inudzuka, Y. Yamazaki, M. Katayama, and K. Oura, Appl. Surf. Sci. **169-170**, 113 (2001).

[19] S. W. King, R. F. Davis, and R. J. Nemanich, Surf. Sci. **603**, 3104 (2009).

[20] F. C. Bocquet, R. Bisson, J. M. Themlin, J. M. Layet, and T. Angot, J. Phys. D: Appl. Phys. **47**, 094014 (2014).

[21] S. W. King, S. Tanaka, R. F. Davis, and R. J. Nemanich, J. Vac. Sci. Technol. A **33**, 05E105 (2015).

[22] See Supplemental Material at http://link.aps.org/supplemental/10.1103/PhysRevB.99.235434 for incomplete silicate adlayer, "moth-eaten" like surface and confirmation of six-fold symmetry.

[23] J. Bernhardt, J. Schardt, U. Starke, and K. Heinz, Appl. Phys. Lett. **74**, 1084 (1999).

[24] W. Lu, P. Krüger, and J. Pollmann, Phys. Rev. B **61**, 13737 (2000).

[25] M. A. Van Hove, W. Moritz, H. Over, P. J. Rous, A. Wander, A. Barbieri, N. Materer, U. Starke, and G. A. Somorjai, Surf. Sci. Rep. **19**, 191 (1993).

[26] G. Kresse and J. Furthmüller, Phys. Rev. B **54**, 11169 (1996).

[27] J. B. Pendry, J. Phys. C **13**, 937 (1980).

[28] J. Schardt, C. Bram, S. Müller, U. Starke, K. Heinz, and K. Müller, Surf. Sci. **337**, 232 (1995).

[29] A. Nakajima, H. Yokoya, Y. Furukawa, and H. Yonezu, J. Appl. Phys. **97**, 104919 (2005).

[30] K. Hayashi, K. Morita, S. Mizuno, H. Tochihara, and S. Tanaka, Surf. Sci. **603**, 566 (2009).

[31] V. Borovikov and A. Zangwill, Phys. Rev. B **79**, 245413 (2009).

[32] X. Chen and Y. Li, Surf. Sci. **681**, 18 (2019).

[33] U. Starke, J. Schardt, and M. Franke, Appl. Phys. A **65**, 587 (1997).

[34] U. Starke, C. Bram, P. R. Steiner, W. Hartner, L. Hammer, K. Heinz, and K. Müller, Appl. Surf. Sci. **89**, 175 (1995).

[35] F. Owman and P. Mårtensson, Surf. Sci. **330**, L639 (1995).

[36] L. I. Johansson, F. Owman, and P. Mårtensson, Phys. Rev. B **53**, 13793 (1996).

[37] U. Starke, Phys. Status Solidi B **202**, 475 (2001).

[38] K. Arima, K. Endo, K. Yamauchi, K. Hirose, T. Ono, and Y. Sano, J. Phys.: Condens. Matter **23**, 394202 (2011).